Innovative robot for chamomile flower harvesting as a new approach based on visual selection

Gamal E. M. Nasr [1], Mohamed M. Ibrahim [1*], Mohamed Y. Tayel [2], Dina S. Salama [2*]

*(1. Agricultural Engineering Department, Faculty of Agriculture, Cairo University, 12613, Egypt;
2. Water Relation and Field Irrigation Department, Agricultural and Biological Research Institute, National Research Centre, 12622, Egypt)*

Abstract: One of the most significant crops, the production of which the Egyptian government tends to increase, is chamomile flowers. In contrast, the expansion of this crop's agriculture is being driven by the high cost of manual harvesting. The goal of this study was to design and test a robot that could harvest chamomile flowers while preserving the plant's health, cutting costs, and maintaining flower quality. A prototype of chamomile flower harvesting robot was designed, manufactured and tested. The robot consists of three main systems: the mobile platform, the delta mechanism, and the visual selection system which detects the flowers ready for harvesting. The flower quality and technical evaluation criteria were the two primary evaluation factors. An overall evaluation criterion for manual harvesting and harvesting robots was also calculated in order to compare the two harvesting systems. The chamomile robot could achieve a cycle time of 3 s and harvest time 21 s/plant. During the harvest season, the robot produced 1200 flowers/hour with an average harvest success 75% - 89%. Three aspects of the robot's visual system were examined: detection ability, accuracy, and detection precision ratio. The outcomes demonstrated that the robot could achieve an accuracy of 72.4% and a detection precision ratio of 75%. For the flower quality criterion, the majority of the flower samples gathered by the robot fell into the high-quality and medium-quality flower categories. According to the overall endpoint results, the robot outperformed manual harvesting (23.53%) in terms of percentage (80%).

Keywords: robot, harvesting, chamomile**,** visual selection, evaluation

Citation: Nasr, G. E. M., M. M. Ibrahim, M. Y. Tayel, and D. S. Salama. 2024. Innovative robot for chamomile flower harvesting as a new approach based on visual selection. Agricultural Engineering International: CIGR Journal, 26(4):261-275.

1 Introduction

Since at least 5,000 years ago, herbs have played a significant role in both conventional and alternative medical treatments (Srivastava et al., 2010). In addition, medicinal plants are also used for the production of teas, extracts, tinctures, food supplements, and natural colors. They are also often used in the food industry, varnishes and paints, cosmetics, as well as for the ecological restoration of paintings (Woldeab et al., 2018). Chamomile is considered one of the most important and valuable plants in the medicinal and aromatic plant exporting market and is widely utilized in numerous industries (Ivanović et. al., 2014). Egypt is one of the chief producers' countries within the production of

Received date: 2023-12-21 **Accepted date:** 2024-10-01

***Corresponding author: Dina Saber Salama,** Researcher, 33 ElBehoous St. Dokki. Giza, Egypt, +20 01003656863, dina.saber@ymail.com.

Mohamed M. Ibrahim, Professor of Agricultural Engineering, Faculty of Agriculture, Cairo University Rd, Al Giza, Giza Governorate, Egypt, +20 1142698112, mohamed.ibrahim@agr.cu.edu.eg.

chamomile, as it occupies second place after Argentina, taken after Germany, France, Italy, Turkey, Greece, Bulgaria, Yugoslavia, Hungary, Slovakia, and Australia (Prasad, 2021). Egyptian chamomile has great popularity in the global export markets due to the quality of its flower heads and the application of organic farming systems (Shalaby et al., 2010). Currently, however, chamomile flowers are mainly harvested manually. The high cost of manual harvesting, in addition to the lack of labor required to conduct it, is considered one of the most important problems facing chamomile production and impeding the expansion of its cultivation in Egypt. Many studies have been conducted to develop mechanical harvesting of chamomiles (Vangeyte et al., 2008), Portable machines (Radwan et al., 2015), and harvesting tools, but harvested flower quality remains the determining criterion for the applicability of this type of different harvesting methods.

Over the years, a number of mechanical harvesting methods have been developed in response to the need for chamomile flower mechanical harvesting methods. The development of mechanical chamomile harvesting has been the subject of numerous studies (Vangeyte et al., 2008; Radwan et al., 2015). The several automated methods have also been utilized to harvest chamomile flowers. Extensive research has been conducted with the aim of exploring the implementation of robotic technology in the floral harvesting process. Abarna and Selvakumar (2015) developed flower picking robots, they designed and developed a rose flower picking robot based on image processing to select the flowers to be harvested. In their recent study, Shree et al. (2019) proposed an innovative approach to automatic harvesting through the use of a deep convolutional neural network robotic system. Specifically, the system was designed and implemented for the purpose of detecting flowers to be harvested in an efficient and streamlined manner. Vinoth Kumar et al. (2019) designed and implemented a fully autonomous robotic system capable of collecting flowers. The flowers can be harvested from the plant in perfect condition with the help of the robotic arm cutter, which takes less time to harvest than manual harvesting. Guo et al. (2022) designed a picking robot based on a parallel manipulator to harvest safflower plants. However, other concepts are used for image analysis to compute the best cutting spot, which is then given to a driver who positions a straightforward mechanical cutting mechanism to produce a clean cut.

In the past ten years, deep learning (DL) has received a lot of attention as a tool for computer vision and object detection. Older computer vision techniques perform better than supervised DL technologies (Kamilaris and Prenafeta-Boldú, 2018; Liu et al., 2018). Convolutional neural network-based object and keypoint detectors like YOLO (Redmon et al., 2016) and CenterNet (Zhou et al., 2019) have advanced to the state-of-the-art thanks to these breakthroughs and can now recognize learnt objects in real-time under difficult circumstances. However, large, labelled datasets are frequently needed in order to train supervised DL systems. This is especially true for agricultural applications, where it might be difficult to handle all potential variables, such as changes in lighting, background, object arrangement, the presence of weeds, and plant growth stage. Additionally, this raises the expense of data gathering and puts a stop to the use of DL in agricultural settings (Kamilaris and Prenafeta-Boldú, 2018; Roh et al., 2021).

A unique visual selection-based robot for harvesting chamomile flowers was the primary objective of the current project. The optical system ensured that only blossoms at the appropriate stage of maturity were harvested, protecting the health of the plants and flowers in the process. According to the specified Assessment Criteria, the aforementioned robot's evaluation and testing were conducted. Using these standardized measures, the robot's performance during the harvesting process was examined for effectiveness.

2 Materials and methods

The different steps in the design and use of

chamomile flowers harvesting robot can be divided into three categories: building detection model, design and implement the mechanical parts of the robot, and real time evaluation of the robot. These subdivisions and their corresponding steps are shown in Figure 1.

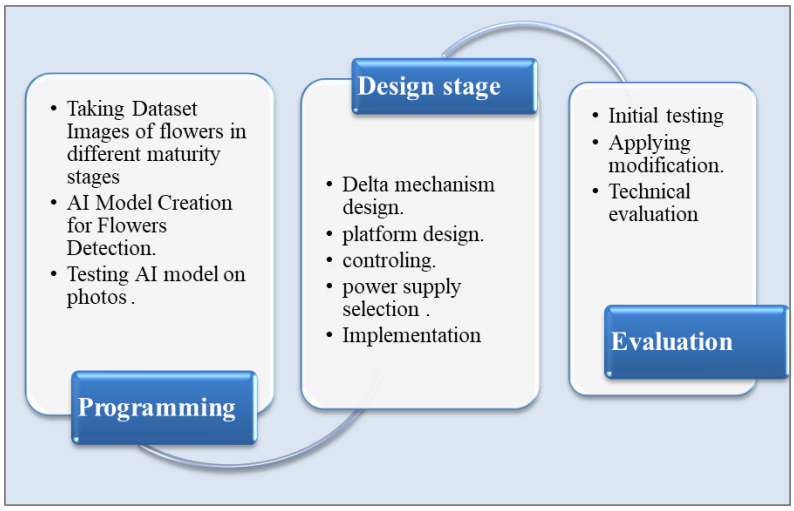

Figure 1 Visualization of the design and use of chamomile flowers harvesting robot: building detection model, design and implement the mechanical parts, and real time evaluation of the robot

2.1 Programming

2.1.1 Detection model building

Dataset of images of chamomile flowers in different maturity stage (Figure 2) captured in an uncontrolled environment to create detection model. The software pipeline of the robot can be divided into three main parts: The AI algorithm detects the flower positions, it then feeds them into the robotics equation to calculate the delta mechanism motion angles, this is transmitted to the low level controller to move the stepper motors and cut the flowers. The low-level controllers also handle robot motion.

2.1.2 Flower detection and classification

The task of classifying flowers is a major reason why artificial neural networks emerged and is the reason why a DL approach was taken. In this research our main goal was to classify mature chamomile flowers, for them to be cut later using extended robotic tools. Generally, this can be done by training a computer on how to differentiate between flowers.

(a)

(a) hole plant, (b) Ideal maturity stage, (c) advanced maturity stage, and (d) early maturity stage

Figure 2 Chamomile flowers in different maturity stage

A data pipeline or data flow, in our case, would typically consist of three phases, as follows:

1. An input device (a camera) is used to capture a snapshot of the flowers.

2. An object detection algorithm is used to find objects in the snapshot and classify and filter mature

chamomile flowers.

3. The algorithm then returns coordinates, these coordinates are then sent to the microcontroller of a parallel embedded system used to control cutting and collecting tools.

For the detection algorithm (YOLOv4) (Bochkovskiy et al., 2020) algorithm was used and implemented in Python and TensorFlow, due to its CPU (Centeral Processing Unite) and GPU (Graphics Processing Unite) performance conservation for real-time application, while also keeping the required high accuracy. A deep convolutional neural network (CNN) is trained to identify object-like parts of the image simultaneously and then predict multiple bounding boxes of the objects. Figure 3 is the architecture of the YOLO CNN

2.2 The prototype design of Chamomile Flower Harvesting Robot (CFHR)

The prototype CFHR components were constructed of two main parts, as illustrated in Figure 4. The first part is the mechanical parts including four-wheel drive metal chassis (moving platform), delta mechanism, and cutting mechanism. The second part is the control system containing Raspberry Pi Camera Module, Nvidia Jetson Nano controller, Arduino UNO, stepper motors, DC motors, motor drivers, power supply, and battery. The prototype of CFHR is shown in Figure 5.

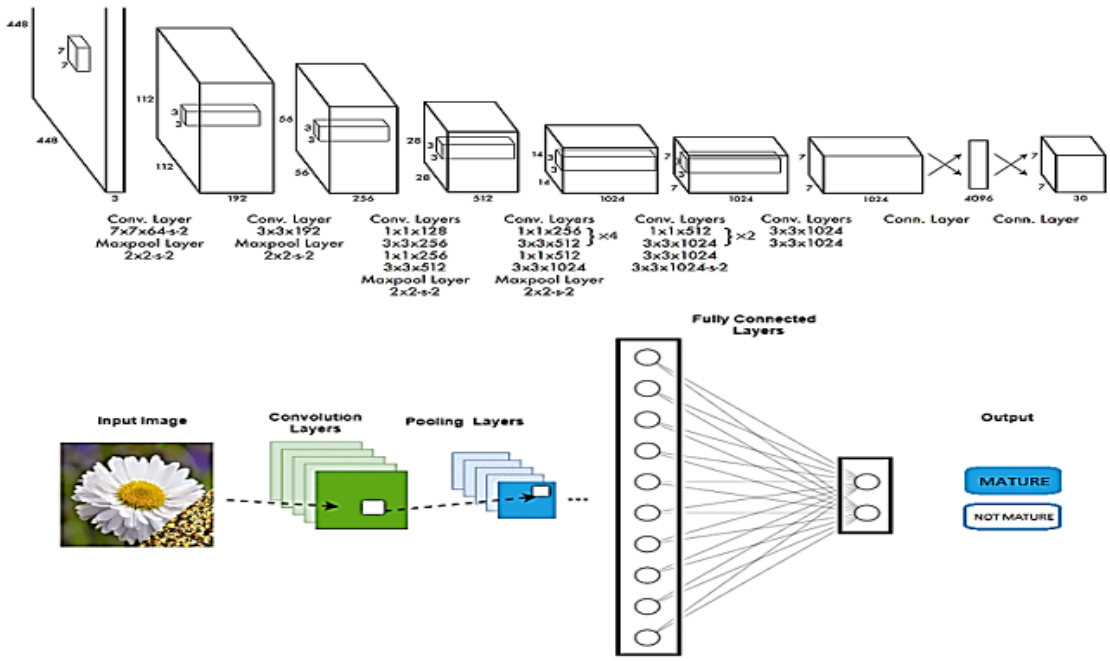

Figure 3 The architecture of YOLO CNN

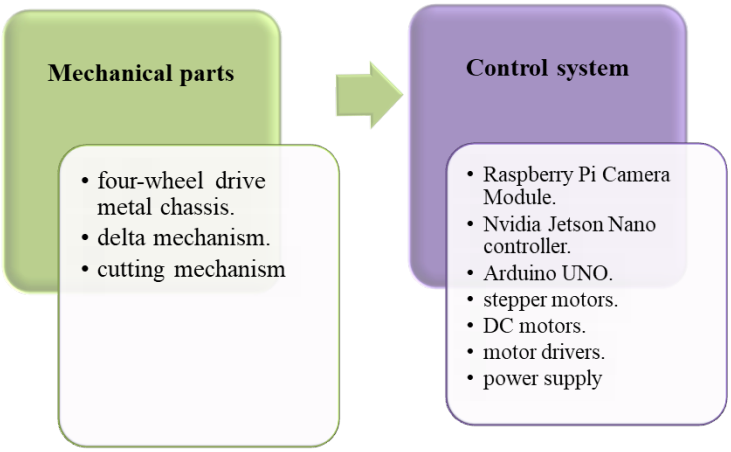

Figure 4 CFHR components

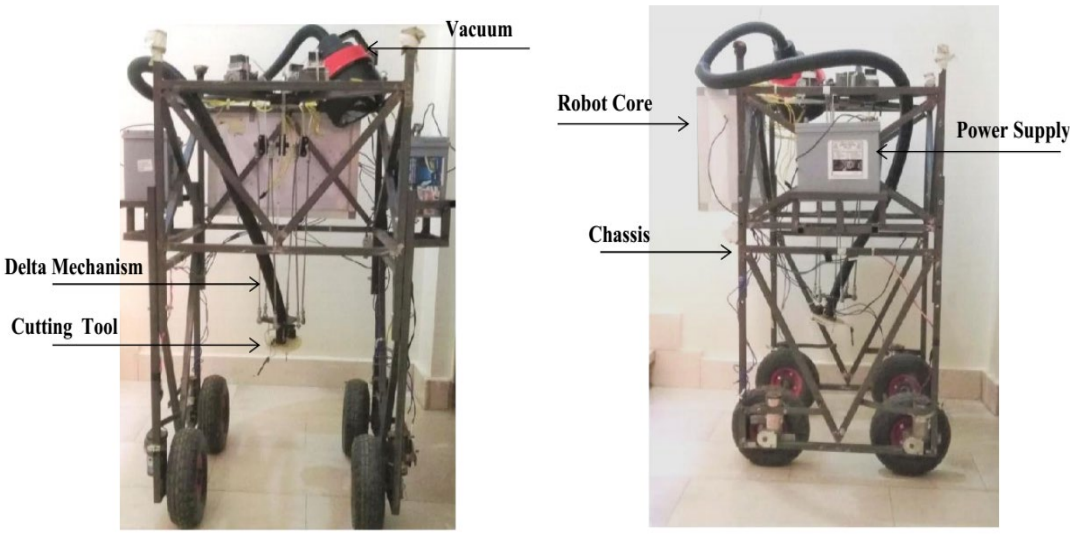

Figure 5 CFHR prototype

2.2.1 Moving platform

The mechanical parts of CFHR design are constructed with Steel square tubes of SAE 304 stainless steel (20 × 20 mm) with 2 mm thickness for the moving platform. The final dimensions of the moving platform were 60 cm × 60 cm with adjustable height of 120 cm. This feature enables the robot to be conveniently maneuvered through a plant environment. Four heavy-duty rubber wheels (10 inch) powered by Four 24 V DC motors were attached to the system frame for easy movement between rows in the farm. A numerical finite element analysis was done on the chosen cross section to confirm the analytical results using ANSYS Mechanical APDL (Figure 6) and the results showed much safer values than the analytical solution.

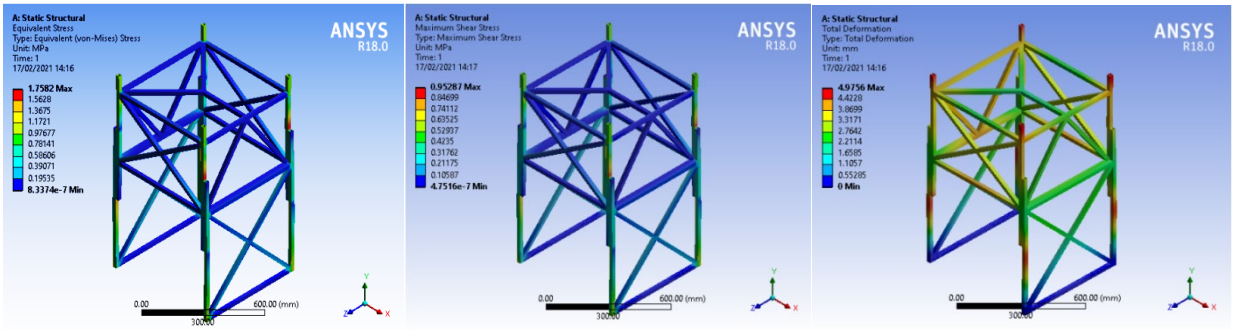

Figure 6 Numerical Finite Element Analysis using ANSYS Mechanical APDL stress analysis results

1. Fix base 2. Input link 3. Revolute joint 4. Forearm 5.Travelling plate 6.Actuator

Figure 7 The delta robot mechanism for picking device,

Table 1 The dimensions of each part of Delta robot

Parameter	Description	value
LA	Length of arm	0.16 m
LB	Length of forearm	0.5 m
RA	Distance from the center of base to the motor joint	0.085 m
RB	Distance from the center of travelling plate to the joint	0.03 m
τ	Motors torque	16 kg cm
X workspace	Workspace in x-direction	0.15 m to 0.15 m
Y work space	Workspace in y-direction	0.15 m to 0.15 m
Z work space	Workspace in z-direction	0.34 m to 0.40 m

To design and control the delta robot a mathematical model is driven through invers and forward kinematics to find a relation between the motors' angles and the end effector position. Another relation is driven by Jacobian matrix between motors' rotational speeds and end effector linear speed. The Kinematics model of delta mechanism includes both inverse kinematics and forward kinematics. The yield equations of inverse kinematics were as follow.

$$l_1^B = \begin{Bmatrix} x \\ y + L\cos(\theta_1) + a \\ z + L\sin(\theta_1) \end{Bmatrix} \quad (1)$$

$$l_2^B = \begin{Bmatrix} x - \frac{\sqrt{3}}{2} L\cos\cos(\theta_2) + b \\ y - \frac{1}{2} L\cos(\theta_2) + c \\ z + L\sin(\theta_2) \end{Bmatrix} \quad (2)$$

$$l_3^B = \begin{Bmatrix} x + \frac{\sqrt{3}}{2} L\cos(\theta_3) - b \\ y - \frac{1}{2} L\cos(\theta_3) + c \\ z + L\sin(\theta_3) \end{Bmatrix} \quad (3)$$

$$a = w_B - u_P \quad (4)$$

$$b = \frac{s_P}{2} - \frac{\sqrt{3}}{2} w_B \quad (5)$$

$$c = w_p - \frac{1}{2} w_B \quad (6)$$

Where , x, y, z are coordinates located within the working space in both directions x, y, and z, L is upper legs length (mm), $\theta_{1,2,3}$ revolute joint angles (degree), W_B is Planar distance from *{0}* to near base side (mm), u_P is Planar distance from $\{P\}$ to a platform vertex (mm), $\boldsymbol{S_P}$ is Platform equilateral triangle side, and W_P is Planar distance from $\{P\}$ to near platform side (mm). Regarding forward kinematics as a result of the translation-only motion of the three degree of freedom delta mechanism, there is a straightforward analytical solution for which the correct solution set is easily chosen. After solving all equations the MATLAB given simulation model for delta motion. A numerical method was carried by using MATLAB R2016B- to determine workspace. In this method, first, kinematic equations are derived. Afterward, applied constraints on joints are considered. Through point by point search in Cartesian space and using kinematic equations, joints variables can be calculated for each point. If these variables satisfy the applied constraints and the determinant of Jacobean is not equal to zero, the point will be distinguished as a part of workspace. Collecting all these points, the robot workspace is determined.

2.2.3 Cutting end effector

The harvesting methodology employed in the chamomile harvesting robot consisted of utilizing linear picking combs complemented by an auxiliary cutting implement for the stalks. The design of the cutting mechanism (Figure 8) has been developed with the primary goal of ensuring the complete inclusion of flowers within the designated cutting area during the cutting process. The process of restricting the chosen flowers within confined parameters was achieved through the utilization of three fundamental components, specifically the duo of cutting blades paired with a comb designed to secure the floral component and facilitate the delivery of incisive action executed at a duration most conducive to optimal harvesting outcomes. This technique proved instrumental in achieving a superior

caliber of selected flowers. The tripartite systems undergo movement facilitated by three servo motors with a maximum torque of 16 kg cm^{-1}.

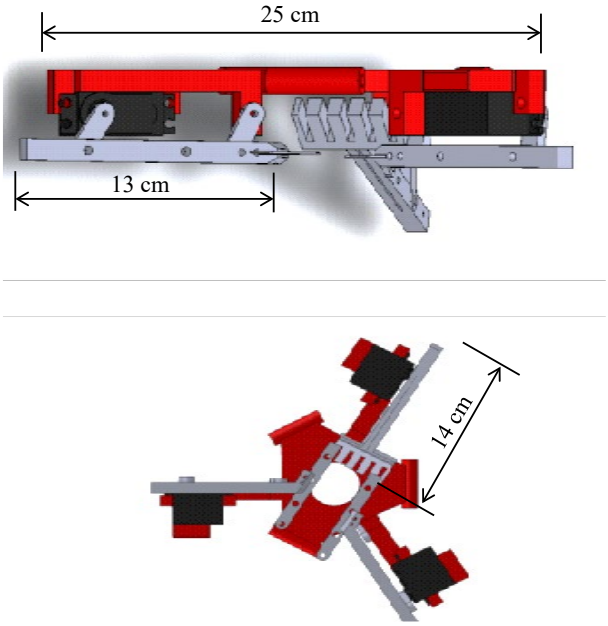

Figure 8 The cutting mechanism

2.2.4 Control system

At the core of the robot, there are two main programmed controllers driving the logic of the robot motion and actions. The first controller is an Arduino Uno device. The Arduino operates on 16 MHz clock and has support for GPIO, PWM and Serial communications which makes it very suitable for this purpose of low-level control. It is responsible for driving the motors by accepting data from the second controller or the remote controller and output the relevant signals to the motor drivers to move the robot or the delta mechanism. The second controller is an Nvidia Jetson Nano. The most important aspect of this controller is that it has a GPU which makes it specifically suitable for the purpose of computer vision and object detection by the help of the added Raspberry Pi V2 Camera connected onboard and the detection algorithm. This controller is responsible for the detection and classification of the chamomile flower as well as carrying out the computations for the delta mechanism due to its powerful onboard computer. The controlling schema illustrated in Figure 9. In order for the robot to function reliably during its operating hours, it is imperative to equip it with a power supply that is both portable and capable of providing the necessary energy output. The Lead-Acid battery has been selected as a viable power supply method. The current draw of the robot was estimated through practical means to be approximately 10 A. Subsequently, a battery with a capacity of 55 A h was selected to enable the robot to operate continuously for more than 5 hours prior to requiring a recharge.

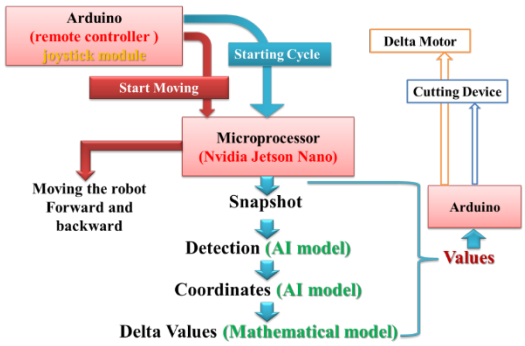

Figure 9 Robot core schema

2.3 Chamomile plants' and flowers' geometric properties

The dimensions of CFHR were designed according to the geometric properties of plants and flowers. The geometric properties were collected from a traditional flower farm at Giza, Cairo, Egypt (29°56'25"N 31°15'00"E), where chamomile plants are planted in rows. The plant height was measured using a meter (m), as well flower distribution.

2.4 Assessment criteria of CFHR

The evaluation of the CFHR rests upon two pivotal parameters, namely, the technical appraisal of the robot itself and the quality of the picked flowers. The evaluation of flower quality stands as a crucial comparative measure that consistently favors manual harvesting over mechanized harvesting within the setting of Egyptian conditions. A random sampling approach was adopted to select a portion of the flowers harvested, with the aim of assessing their quality. Each of these selected flowers was subjected to a meticulous grading process according to Mohr (1993), resulting in the determination of quality grades (Table 2).

Table 2 Quality grades for chamomile flowers

Grade	Specifications
First	Flowers with stem <10 mm,
Second	Flowers with stem 10–30 mm,
Third	Flowers with stem 30–50 mm

Furthermore, the proportion of each quality grade was mathematically computed and compared with manual harvested flowers samples. The assessment of the technological capabilities of the chamomile harvesting robot was centered around a set of fundamental criteria, which pertained to cycle time, harvesting time, production rate, the harvest success ratio, and the visual selection assessment parameter. Pots experiment was carried out to test and evaluate the robot's technical performance criteria. The experiment includes 20 pots (5 rows × 4 pots) with one plant in each pot and medium texture soil. The distance between pots was simulated to the distance between plants in the field (30 cm × 30 cm). Irrigation and fertilization were carried out in accordance with the recommended doses. The aforementioned variables were considered essential in evaluating the efficiency of the robot. To evaluate the visual selection system of chamomile harvesting robot there were three main parameters were used (Detection capability – Accuracy – Detection precision rate %). To calculate the accuracy of the robot there were 4 possible cases according to Yang et al. (2018): True positive (*TP*) is the number of cases that are positive and detected positive. False positive (*FP*) is the number of cases that are negative but detected positive. True negative (*TN*) is the number of cases that are negative and detected negative. False negative (*FN*) is the number of cases that are positive but detected negative

$$\text{The Accuracy (\%)} = TP/(TP+TN) \times 100 \quad (7)$$

Detection precision rate was calculated according to Yang et al. (2018) as follow:

$$\text{Detection precision rate (\%)} = TP/(TP+FP) \times 100 \quad (8)$$

In expansion to these criteria, a comprehensive assessment criterion (overall evaluation criterion) was calculated to compare both manual harvesting and harvesting utilizing robotics to provide a comprehensive view of the assessment. Criterion value was calculated for both manual and robotic harvesting according to Ghonimy et al. (2021), where three basic evaluation criteria (flower quality, production speed and price) were combined to calculate a comprehensive evaluation criterion. The overall evaluation criterion (OEC) was calculated in the following three steps.

1. Organization of evaluation criteria according to their relative weight.

2. Defining a quality attribute for each criterion

3. Calculation of the value of the general evaluation criterion.

Evaluation criteria were selected (quality of harvested flowers, production costs and production speed). The relative weights were chosen after a careful analysis of the relative importance of each evaluation criterion as shown in Table 3. The relative weight of the evaluation criteria was decided based on the nature of the registration process. Harvest flower quality (QHF) had the highest relative weight (40%) because it is considered the most important criteria for chamomile production. Production cost (PC) had the same relative weight (40%) because it represents the main problem in the production process of chamomile under Egyptian conditions. The production rate (PR) was given a lower relative weight (20%) because its values were considered in the calculation of productivity and production costs.

Table 3 Assigned weights of the evaluation criteria

Evaluation criteria	Relative weight (%)
Quality of harvested flowers (QHF)	40
Production cost (PC)	40
Production rate (PR)	20

3 Results

3.1 Chamomile plants' and flowers' geometric properties

The plant height that cultivated under Egyptian conditions exhibit a range between 70cm to 85 cm, whilst the mean dimension amounts to approximately 77 cm. During the peak of the harvest season, the quantity of flower blooms on a single plant varied within the range of 15 - 25 blooms per plant. The investigation examined the arrangement pattern of flowers at the pinnacle of flowering, relative to the vertical dimension of the plant. Measurements were obtained from three different distances, namely 10, 20 and 30 cm, above the apex of the plant. The aforementioned distances were selected since they correspond to the location of the flowers that were deemed suitable for harvest. Through the analysis of the data, it was determined that a majority of the flowers, quantified at 76.22% were situated within the initial 10 cm of the plant's length. Additionally, a smaller percentage of the flowers, amounting to 21.63% were positioned approximately 20 cm from the apex of the plant. The findings also revealed a minimal proportion of flowers, constituting merely 2.15%, located at a distance of 30 cm from the uppermost extremity of the plant (refer to Figure 10 for graphical representation). As evidenced by the data, a majority of the flowers (approximately 88%) are observed to be situated within the uppermost 20 cm region of the plant.

Figure 10 Flower distribution as percentage along plant stem

3.2 Technical aspects testing results

3.2.1 Delta mechanism working space simulation (MATLAP)

The delta robot's working space was simulated to ensure it covered the planned work area by imposing a set of random points with coordinates located within the working space in directions X, Y, and Z. According to the simulation results as shown in Figure 11a, the delta robot was able to cover the working plane Y-Z in the prescribed area (30 cm in the Y direction and 30 cm in the Z direction) as well as in the X-Z plane (Figure 11b). The simulation results (Figure 11c) demonstrated that the delta robot covers the working space designed to cover it by covering the X-Y plane in accordance with the designed work circle (30 cm diameter).

3.2.2 Cycle time and harvesting time

According to the testing results, CFHR recorded constant value of cycle time with 3 seconds. The previous researches results showed that wide variance in cycle time values for different types of flowers harvesting robots. Wu et al. (2022) recorded cycle time for *Camellia oleifera* flowers as 1.2 seconds, while Guo et al. (2022) recorded 16 seconds cycle

time for *safflower* harvesting robot. By good observation of researches results it could be cleared that type, size, physical and mechanical properties of the plant may be the reason of cycle time variation as well as the appropriate harvesting method. This explains the value of cycle time for chamomile flowers harvesting robots, as the flowers are sensitive and its stems have small diameter. As for the harvesting time, it was calculated during the three harvest times for each of (one pot - a row of pots - the entire experiment). Table 4 shows the distinctive values of harvest time during the three harvests. The robot was able to attain an average harvesting time for one pot of 21 seconds, whereas the average time required to harvest a row of pots was 84.18 s seconds. The harvest time for the complete experiment included the times lost in turning and moving through rows and the times taken to fix technical absconds during operation. The robot was able to achieve the average harvesting time for the entire experiment of 13.88 minutes. Crop characteristics, the nature of the vegetative development, the cover and dispersion of flowers or fruits on the plant, this factors significantly influence the collect process, as they have an impact on the speed of detection and separation (Edan et al., 2000; Gu et al., 2012; Yaguchi et al., 2016; Bac et al., 2017; Xiong et al., 2020). It is possible to explain the increase in harvesting time as a result of the increase in the rate of flowering and the vegetative growth, in addition to the overlapping between plants and the flowers locations on the plant.

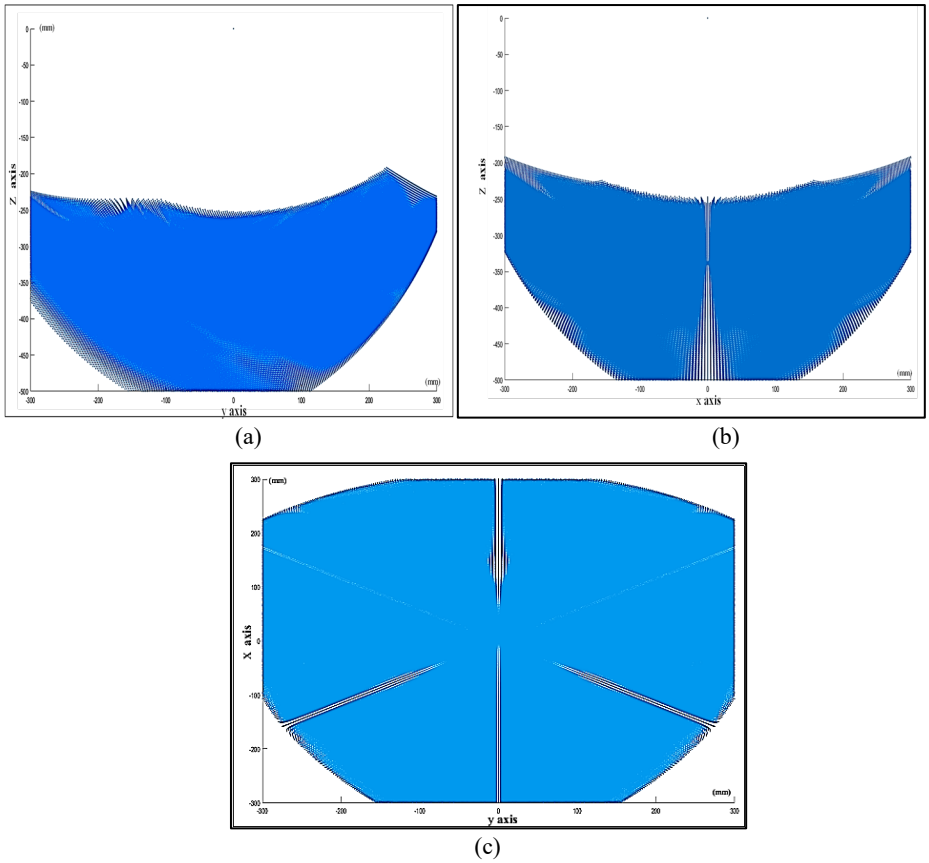

(a) (b)

(c)

Figure 11 Delta mechanism working space simulation (MATLAP)

Table 4 Harvesting times for CFHR during harvesting season

Parameter	Harvest times			
	1st	2nd	3rd	Average
Harvesting time for one plant (sec)	13	22	28	21
Total harvesting time for pots line (sec)	52.15	88.20	112.20	84.18
Flower numbers (one plant)	4	7	9	6
Total harvesting time for experimental plot (min)	10.35	13.95	17.35	13.88

3.2.3 Harvesting success ratio and production rate

The results of measuring the harvesting success ratio criterion for the chamomile robot are shown in (Table 5). During the harvest season, estimations

were taken for three harvest times (first, second and third harvests). During the three harvest times, chamomile robot recorded a success ratio of 75% within the first harvest and 85.7% within the second. Whereas the third harvest had the most noteworthy success ratio of 89.7%. By perception of flower harvesting robots research results it can be found that the harvest success ratio for these robots ranges from 80% to 96%. Gerbera Jamesonii harvesting robot recorded harvesting success ratio 89.7% whereas Rosa Damascene harvesting robot had harvesting success ratio 82.22% (Kohan et al., 2011; Rath and Kawollek, 2009). Safflower harvesting robot recorded harvesting success ratio 87.91% (Guo et al., 2022) and the most noteworthy harvesting success ratio was recorded by Camellia oleifera Flowers harvesting robot and it was 96% (Wu et al., 2022). It is obvious that the increment within the success ratio can be ascribed to the increment in plant density and flowering rate during the harvest season. The production rate of chamomill harvesting robot was recorded as 1200 flowers/hour. The production rate also expressed in g h^{-1} and it was 24.86 g h^{-1}.

Table 5 Harvesting success ratio for chamomile robot during harvesting season

Harvesting times	Harvest success ratio %
First	75.0
Second	85.7
Third	89.7

3.2.4 The visual assessment parameters

The chamomile robot's visual selection system was judged based on two important factors (accuracy % and detection precision rate %). These factors were checked three times during harvesting season (first, second, and third harvest times) and it's shown in Table 6 and Figure 12. The comes about of the precision basis varied concurring to the distinctive harvest times. The robot was able to realize an accuracy of 72.4% within the to begin with collect, and 59.5% within the second harvesting whereas the most reduced esteem was recorded within the third time of harvesting, and it was 53.9%. The reason can be attributed to the low accuracy due to the increase in plant density, which makes it difficult to accurately detect the flowers ready for harvest, as well as the different locations of the flowers on the plant, where the robot was able to detect the clear flowers, while finding it difficult to find other flowers. The quality of the image and lighting often affected the accuracy of the discovery and selection of flowers. The comes about of the detection precision rate showed that the robot was able to realize an average detection precision rate of 75% for the first harvesting and 50% for the second, whereas its least esteem was within the third time, which summed to 49.7%. Table 7 showed the parameters values that included in the overall evaluating criterion (OEC) calculation for the harvesting methods of chamomile (robot and manual). The quality characteristic (QC), worst value (WV), target value (TV), and relative weight (RW) of the evaluating criteria were shown in Table 8.

Table 6 Visual selection evaluating parameters for CFHR

Visual selection evaluating parameters	Harvesting times		
	1st	2nd	3rd
Accuracy %	72.4	59.5	53.9
Detection precision rate %	75.0	50.0	49.7

Table 7 The average values of evaluating criteria for different harvesting methods (Robot, Manual, and Mechanical)

Parameters	Robot	Manual
Quality of harvested flowers (%)*		
First	78.3	65.04
Second	21.7	33.65
Third	NF**	1.31
Production cost (EGP/fed.)	9813.74	10250
Production rate (Kg h^{-1})***	0.025	1.5

Note: * Quality of harvested flowers for the robot is the average values for each grade during the three harvesting time

** NF means no flowers recorded in this grade.

*** Production rate for manual harvesting was calculated according fielding data.

(a) first harvest time, (b) second harvest time, (c)third harvest time

Figure 12 Detection Images for CFHR

Table 8 Values of evaluating criteria related to the overall evaluation criterion

Evaluation criteria	Worst Value	Target Value	Quality characteristics	Relative weight (%)
Quality Of Harvested Flowers (QHF) (%)*	45.84%	78.3%	Higher	40
Production Cost (PC) (EGP/Fed.)	21392.7	9813.74	Lower	40
Production Rate (PR) (Kg/h)	0.025	34.8	Higher	20

Note: *The percentage of harvested flowers in first grade.

These values were used to calculate the contribution of the evaluating criteria into the OEC. The maximum and minimum values for each evaluating criterion were considered to represent the values of Wv and Tv, respectively.

Table 9 Values of the overall evaluation criterion

Harvesting Method	OEC (%)
Robot	80
Manual	23.53

Table 9 shows the overall evaluation criterion for CFHR and manual harvesting. The estimated values of OEC showed that CFHR achieved the higher value 80% comparing with manual harvesting which recorded 23.53%. Looking closely at the results, it is clear from the OEC results that the use of robots is the best choice for chamomile harvesting, due to its higher percentage (80%) comparing with the manual harvesting under Egyptian conditions. The high result of the OEC for the robot can be explained due to the relative weight of both quality of harvested flowers and production costs, as the robot achieved high quality of harvested flowers and lower production costs.

3.3 Flower quality parameter

Flower quality criterion (Figure 13) indicated that CFHR achieved a high degree of flower quality during the three collection times. Flower quality degree was between high and medium (Figure 14) compared with manual collection, which included three degrees of flower quality. High-quality flower rate was (78.6%, 77.8%, and 78.5%) for the first, second, and third collection times, respectively, in chamomile robot flower samples. The extent of the medium quality degree of flowers were (21.4%, 22.2%, and 21.5%) for first, second and third harvesting times respectively. The manual harvesting accomplished three degrees of flower quality amid the three harvesting times. Flower quality rates of (64.34%, 34.36%, and 1.3%) for high-, medium-, and low-quality flowers were recorded in the first harvest. The percentages of flower quality within the second harvest were (65.32%, 33.42%, and 1.26%) for high-, medium-, and low-quality flowers, respectively. For the third collection, the rates of flower quality were

66.47% for high-quality flowers, 33.17% for medium quality, and 1.36% for low quality. The robot predominance over manual collection within the flower quality basis is due to the precise design of the cutting device. The cutting distance was set to 10 mm of the flower stem which achieved high quality flowers.

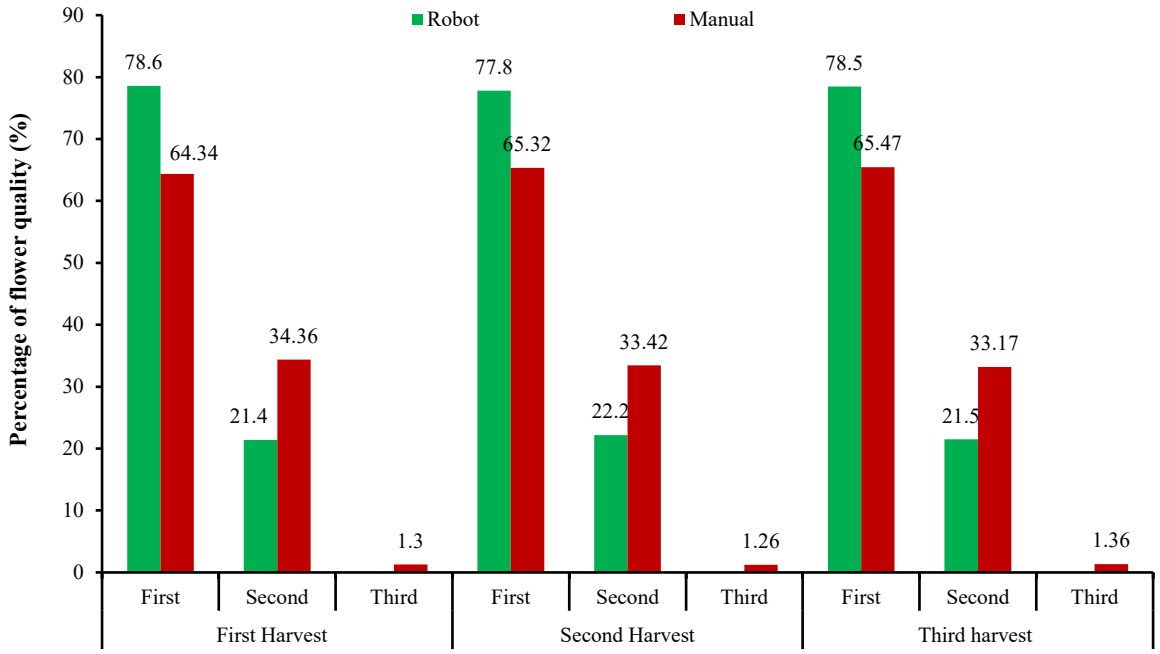

Figure 13 Comparison between CFHR and Manual harvesting with regards of Flower quality percentage

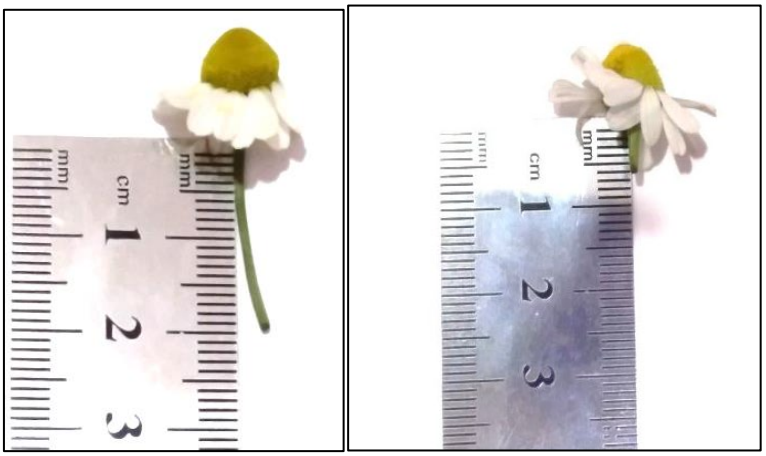

Figure 14 CFHR harvested flowers categories

4 Conclusion

The findings demonstrated that the chamomile harvesting robot can be an effective method for addressing the issue of the high cost of manual harvesting. It is one of the viable mechanical solutions, but it requires further development. Although the results of technical performance indicators are acceptable given that they are in the experimental stage, they require further development. In addition to attempting to achieve higher rates of success in the chamomile harvest process, future studies must focus on achieving high productivity, greater accuracy, and higher time efficiency. The field of agricultural field robots remains one of the promising areas that require additional research.

References

Abarna, J., and A. Selvakumar. 2015. Rose flower harvesting robot. *International Journal of Applied Engineering Research*, 10(55): 4216 – 4220.

Bac, C. W., J. Hemming, B. A. J. van Tuijl, R. Barth, E. Wais, and E. J. van Henten. 2017. Performance evaluation of a harvesting robot for sweet pepper. *Journal of Field*

Robotics, 34(6): 1123–1139.

Bochkovskiy, A., C. Y. Wang, and H. Y. M. Liao. 2020. Yolov4: Optimal speed and accuracy of object detection. *arXiv preprint arXiv*: 2004.10934.

Edan, Y., D. Rogozin, T. Flash, and G. E. Miles. 2000. Robotic melon harvesting. *IEEE Transactions on Robotics and Automation*, 16(6): 831-835.

Ghonimy, M. I., M. M. Ibrahim, A. Ghaly, and E. N. Abd El Rahman. 2021. Performance evaluation of hand-held olive harvesters. *Agricultural Engineering International: CIGR Journal*, 23(4): 127-137.

Guo, H., D. Luo, G. Gao, T. Wu, and H. Diao. 2022. Design and experiment of a safflower picking robot based on a parallel manipulator. *Engenharia Agrícola*, 42(1): e20210129.

Gu, B., C. Ji, H. Wang, G. Tian, G. Zhang, and L. Wang. 2012. Design and experiment of intelligent mobile fruit picking robot. *Transactions of the Chinese Society for Agricultural Machinery*, 43(6): 153-160.

Ivanović, S., M. Pajić, and T. Marković. 2014. Economic effectiveness of mechanized harvesting of Chamomile. *Economics of Agriculture*, 61(2): 319-330.

Kamilaris, A., and F. X. Prenafeta-Boldú. 2018. Deep learning in agriculture: A survey. *Computers and Electronics in Agriculture*, 147: 70-90.

Kohan, A., A. M. Borghaee, M. Yazdi, S. Minaei, and M. J. Sheykhdavudi. 2011. Robotic harvesting of rosa damascena using stereoscopic machine vision. *World Applied Sciences Journal*, 12(2): 231-237.

Liu, A., W. A. Zhang, L. Yu, H. Yan, and R. Zhang. 2018. Formation control of multiple mobile robots incorporating an extended state observer and distributed model predictive approach. *IEEE Transactions on Systems, Man, and Cybernetics: Systems*, 50(11): 4587-4597.

Mohr, T. 1993. Untersuchung und Weiterentwicklung einer selbstfahrenden Arbeitsmaschine zur Pflücke von Blüten ausgewählter Heilpflanzenarten und deren Vergleich mit einer in der ehemaligen DDR zugelassenen Pflückmaschine sowie mit der Handpflücke. Ph. D. diss., Justus-Liebig-Universität Gießen.

Prasad, B. T. 2021. Performance of medicinal and aromatic chamomile (*Matricaria chamomilla* L.) under different planting, manure cum fertilizer regimes in Kathmandu valley. *Journal of Agricultural Science and Technology*, B(11): 26-45.

Radwan, H. A., T. H. Mohamed, and A. O. Elashhab. 2015. Design a machine for picking Chamomile to suit the small holding. *Egyptian Journal of Agriculture Research*, 3(5): 405-425.

Rath, T., and M. Kawollek. 2009. Robotic harvesting of Gerbera Jamesonii based on detection and three-dimensional modeling of cut flower pedicels. *Computers and Electronics in Agriculture*, 66(1): 85-92.

Redmon, J., S. Divvala, R. Girshick, and A. Farhadi. 2016. You only look once: Unified, real-time object detection. *In Proceedings of the IEEE Conference on Computer Vision and Pattern Recognition*, 779-788. Las Vegas, NV, USA, 27–30 June 2016.

Roh, S., J. I. Park, G. Y. Kim, H. J. Yoo, D. Nickel, G. Koerzdoerfer, J. Sung, J. Oh, H. D. Chae, S. H. Hong, and J. Y. Choi. 2023. Feasibility and clinical usefulness of deep learning-accelerated MRI for acute painful fracture patients wearing a splint: A prospective comparative study. *Plos ONE*, 18(6): e0287903.

Shalaby, A. S., S. F. Hendawy, and M. Y. Khalil. 2010. Evaluation of some chamomile cultivars introduced and adapted in Egypt. *Journal of Essential Oil Bearing Plants*, 13(6): 655-669.

Shree, C., R. Kaur, S. Upadhyay, and J. Joshi. 2019. Multi-feature based automated flower harvesting techniques in deep convolutional neural networking. In *Proceedings of 4th International Conference on Internet of Things: Smart Innovation and Usages (IoT-SIU)*, (pp.1-6). Ghaziabad, India. 18-19th April 2019.

Srivastava, J. K., E. Shankar, and S. Gupta. 2010. Chamomile: A herbal medicine of the past with a bright future. *Molecular Medicine Reports*, 3(6): 895-901.

Vangeyte, J., J. Baro, J. Rijckaert, K. Vanden Hautte, W. D'HAESE, and B. Sonck. 2008. Study, design and development of a low-budget prototype harvesting machine for Roman Chamomile. In *2nd International Scientific symposium farm machinery and process management in sustainable agriculture, International Conference on Agricultural Engineering, Hersonissos*, 153-159. Crete, Greece, 23-25 June 2008.

Vinoth Kumar, A., V. Kannarasu, S. Padmapriya, N. Partheeban, and S. Arun. 2019. Design and implementation of autonomous flower harvester using image processing. *International Journal of Recent Technology and Engineering (IJRTE)*, 8(2): 2638-2642.

Woldeab, B., R. Regassa, T. Alemu, and M. Megersa. 2018. Medicinal plants used for treatment of diarrhoeal related diseases in Ethiopia. *Evidence-Based Complementary and Alternative Medicine*, 2018(1): 4630371.

Wu, Z., L. Li, Q. Zhao, X. Guo, and J. Li. 2022. Design and research of a harvesting actuator for *Camellia oleifera* flowers during the budding period. *Agriculture*, 12(10):

1698-1714.

Xiong, Y., Y. Ge, L. Grimstad, and P. J. From. 2020. An autonomous strawberry-harvesting robot: Design, development, integration, and field evaluation. *Journal of Field Robotics*, 37(2): 202-224.

Yaguchi, H., K. Nagahama, T. Hasegawa, and M. Inaba. 2016. Development of an autonomous tomato harvesting robot with rotational plucking gripper. In *2016 IEEE/RSJ International Conference on Intelligent Robots and Systems (IROS)*, 652-657. Daejeon, Korea (South), 09-14 October 2016.

Yang, Q., D. Xiao, and S. Lin. 2018. Feeding behavior recognition for group-housed pigs with the Faster R-CNN. *Computers and Electronics in Agriculture*, 155: 453–460.

Zhou, X., D. Wang, and P. Krähenbühl. 2019. Center Net: objects as points. In *Proceedings of the IEEE Conference on Computer Vision and Pattern Recognition*, pp. 16-20. Long Beach, CA, USA, 15-20th June 2019.